Clays and Clay Minerals, Vol. 53, No. 4, 361–371, 2005.

CLAY-PORPHYRIN SYSTEMS: SPECTROSCOPIC EVIDENCE OF TMPyP PROTONATION, NON-PLANAR DISTORTION AND MESO SUBSTITUENT ROTATION

PATRÍCIA MOURA DIAS, DALVA LÚCIA A. DE FARIA AND VERA R. LEOPOLDO CONSTANTINO*

Departamento de Química Fundamental, Instituto de Química, Universidade de São Paulo, Av. Prof. Lineu Prestes 748, São Paulo SP, Brazil, CEP 05508-900

Abstract—The interaction of the water-soluble 5,10,15,20-tetrakis(1-methyl-4-pyridyl)-21*H*,23*H*-porphine (TMPyP) with different 2:1 phyllosilicates was examined by Raman and UV-visible spectroscopies. The clay samples were saturated with the tetracationic porphyrin and isolated from the aqueous suspension. A red shift of the Soret band was observed for all the clay-TMPyP systems in the order vermiculite < Laponite < mica-smectite (Syn-1) < montmorillonite (SWy-2). Furthermore, three components were observed for the Soret band (at ~425, 455 and 488 nm). Raman spectra of the isolated solids excited at 457.9 nm, 488.0 nm and 514.5 nm suggest the occurrence of porphyrin protonation, non-planar distortion and rotation of the meso substituent. Based on the vibrational data, an acidity scale was proposed for the clays: vermiculite < Laponite < SWy-2 < Syn-1. The relative contribution of the protonated spectra is larger at 457.9 nm than at 488.0 nm, suggesting that the peak at 455 nm corresponds to the protonated species. In Laponite, the relative intensity of the meso substituent band at ~1635 cm^{-1} indicates that the dihedral angle formed between the porphyrin and the methyl-pyridyl rings decreased in the non-protonated porphyrin as a consequence of intercalation. Raman data are thus consistent with the presence of at least two porphyrin species in resonance at 457.9 nm: the protonated and a more planar non-protonated porphyrin. At 488.0 nm the number of enhanced modes increases suggesting a decrease in the porphyrin symmetry. This allows assignment of the absorption band centered at 488 nm to a non-planar porphyrin conformation.

Key Words—Intercalation, Laponite, Mica-smectite Syn-1, Montmorillonite SWy-2, Porphyrin, Raman Spectroscopy, Tetramethylpyridylporphyrin, TMPyP, UV-visible Spectroscopy, Vermiculite.

INTRODUCTION

The interaction between guest species intercalated in layered host structures can produce significant and interesting modifications in chemical, catalytic, electronic, optical and/or mechanical properties of both guest and host species. The isolation of materials with attractive properties *via* soft chemistry routes has allowed the technological and industrial applications of such intercalation compounds as electrochemical components and heterogeneous catalysts (Rouxel *et al.*, 1994; Alberti and Costantino, 1996).

One of the most studied systems from the point of view of intercalation chemistry is the expandable clay mineral group. Porphyrins are among the various species used for intercalation studies on smectites (Figure 1a). These are macrocyclic molecules containing four pyrrole groups linked by methine bridges and are responsible for important biological processes such as molecular oxygen transport and storage, solar energy conversion to chemical energy, and enzymatic reactions (Milgrom, 1997). As dyes, these macromolecules may be used as probes to investigate physicochemical phenomena involving clay minerals as their properties can change as a consequence of the environment.

The first studies of clay-porphyrin interactions were motivated by the occurrence of porphyrins in sediments and petroleum deposits (Kaufherr *et al.*, 1971; Kosiur, 1977; Baker and Palmer, 1978; Bergaya and van Damme, 1982). Later works focused on the reactivity of metalloporphyrins in the clay interlayer region (Bedioui, 1995; Ukrainczyk *et al.*, 1995; Chibwe *et al.*, 1996; Martinez-Lorente *et al.*, 1996).

The porphyrin orientation, the possibility of protonation, metallation (free bases) or demetallation (metalloporphyrins) processes and also modifications in the electronic and/or structural configuration of these macromolecules in the presence of clays have been analyzed employing primarily X-ray diffraction (XRD) and absorption or diffuse reflectance (DR) spectroscopies in the UV-visible area of the spectrum. Other techniques such as infrared (IR) spectroscopy, electron spin resonance (ESR), thermal analysis (TA) and X-ray absorption spectroscopy (XAS) have been used more rarely (Cady and Pinnavaia, 1978; Van Damme *et al.*, 1978; Ukrainczyk *et al.*, 1994; Giannelis, 1990; Carrado *et al.*, 1992; Carrado and Wasserman, 1996).

Clays can be employed in porphyrin synthesis. Studies concerning the synthesis of meso-tetraalkylpor-

* E-mail address of corresponding author:
vrlconst@iq.usp.br
DOI: 10.1346/CCMN.2005.0530404

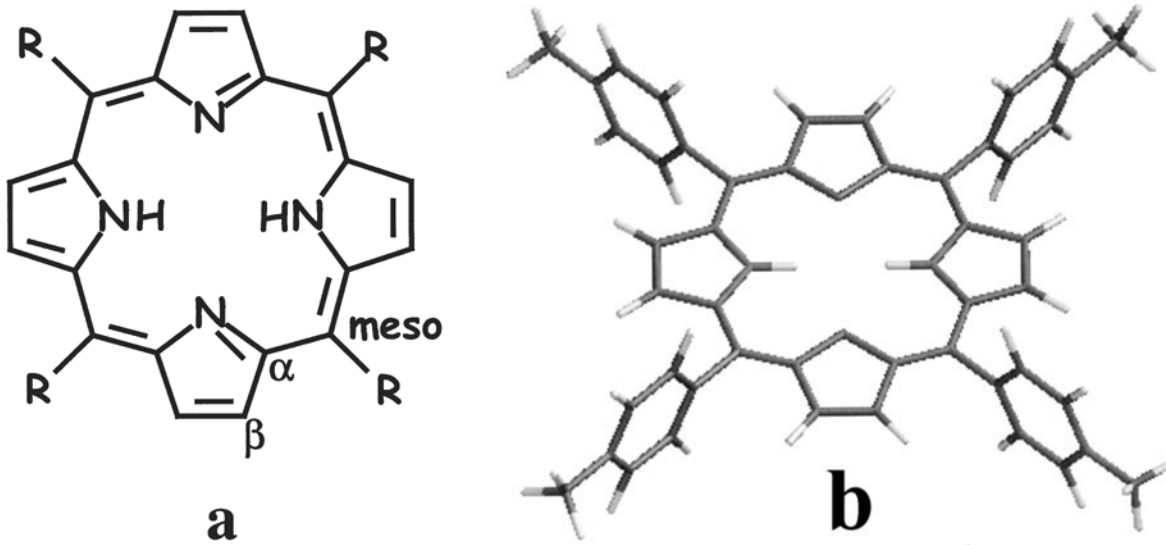

Figure 1. Schematic representations of (a) porphine and (b) TMPyP, where R = 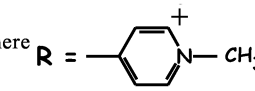

phyrins from aldehydes and pyrroles using clays such as montmorillonite K10 as catalysts were performed, and the reactivity compared with those of homogeneous catalysts (Onaka *et al*., 1993).

Investigations of the characterization of both free base and metallated cationic porphyrins in aqueous clay colloidal dispersions have also been reported (Kuykendall and Thomas, 1990; Chernia and Gill, 1999), where the spectroscopic changes in the visible region were discussed in terms of the porphyrin ring protonation and rotation of the meso-substituted group. Recently, papers on the preparation of clay dispersions containing porphyrins have been published (Takagi *et al*., 2002a, 2002b) showing that the dye aggregation is negligible, thus opening the possibility of using these molecules to explore photochemical energy-transfer processes.

Regardless of the application, detailed knowledge of the changes induced in the guest species by the inorganic matrix is of great importance as chemical reactivity is affected by such changes. In the case of porphyrins, electronic absorption spectroscopy is the most extensively used technique due to the strong absorption bands in the visible region. It is impossible, however, to identify unequivocally the chromophoric species solely from the electronic spectrum data, as the bands are not specific. The tetracationic 5,10,15,20-tetrakis(1-methyl-4-pyridyl)-21*H*,23*H*-porphine (TMPyP, Figure 1b) is a water-soluble porphyrin that has been used in several studies of intercalates. When interacting with clays, the porphyrin Soret band presents a shift to longer wavelengths (red shift) but the reason for such behavior is the subject of some debate. In the case of the LPN-TMPyP system, for instance, the red shift led Kuykendall and Thomas (1990) to conclude that the porphyrin was protonated at the LPN surface, whereas Chernia and Gill (1999) used the same fact to propose *Me*Py rotation towards the porphyrin ring, instead of protonation.

Aiming to address this question, in the present work, TMPyP was intercalated in different 2:1 clays (smectites and vermiculite) and investigated using electronic and resonance Raman spectroscopies. Vibrational spectroscopy (Raman and IR) is much more convenient to characterize the chemical species present in the system than electronic spectroscopy, as atomic vibrations are more sensitive to molecular structure than electronic transitions. The IR spectra of clay-porphyrin systems, however, are dominated by intense bands arising from the inorganic structure, while the Raman spectra are nearly free from such interference. Furthermore, when excited with a laser line that is absorbed by the sample, a selective intensification of several orders of magnitude is observed for the vibrational modes involving the chromophoric group (resonance Raman effect) (Albrecht, 1961). This behavior is particularly interesting when the guest species is an intensely colored molecule such as porphyrins. The resonance Raman technique is sensitive to porphyrin symmetry distortions (Unger *et al*., 1997; Shelnutt *et al*., 1991), electronic distribution perturbations (Sun *et al*., 1997) and changes in properties associated with the molecular environment (Drain *et al*., 1998).

We have demonstrated in a previous study (Dias *et al*., 2000) the possibility of using Raman spectroscopy to investigate protonation and metallation-demetallation processes emerging from clay-porphyrin interaction. Here, the above-mentioned spectroscopic techniques were used in order to obtain a better understanding of the nature of the guest-host interaction and to identify the chemical species present in the system thus helping to clarify the controversy in the literature concerning the

https://doi.org/10.1346/CCMN.2005.0530404 Published online by Cambridge University Press

origin of the red shift observed for the Soret band in the porphyrin intercalates.

EXPERIMENTAL

Materials and methods

In this work four different clays were used. The Clay Minerals Society supplied the natural montmorillonite SWy-2 and the synthetic mica-smectite Syn-1. We also used synthetic Laponite XLS (LPN), supplied by Laporte Inorganics, UK. The designation XLS accounts for the treatment of this Na-hectorite clay with a dispersion agent ($Na_4P_2O_7$) which permits stable high-concentration dispersions (up to 8 wt.%) to be prepared (Laporte, technical directory). A natural vermiculite (VMC) from Paulistana, Piauí State, northern Brazil, found in nature as a macrocrystal, was also used. The chemical analysis of major elements present in VMC was reported by Coelho (1986) as follows: 31.5% SiO_2, 10.60% Al_2O_3, 12.60% MgO, 6.60% Fe_2O_3, 0.50% FeO, 10.90% CaO, 1.30% Na_2O, 1.10% K_2O, 22.70% H_2O^+.

Free-base 5,10,15,20-tetrakis(1-methyl-4-pyridyl)-21*H*,23*H*-porphine (TMPyP) was purchased from MidCentury (Posen, Illinois, USA) as the chloride salt and used as received. This compound was characterized by elemental analysis (CHN), thermal gravimetric analysis (to evaluate the water content), UV-visible and IR spectroscopies. The following data were found: 55.8% C, 5.37% H, 11.8% N, 15.2% H_2O (C/N molar ratio = 5.5); calculated (considering the formula $C_{44}H_{38}N_8Cl_4{\cdot}8H_2O$): 54.8% C, 5.64% H, 11.6% N, 15.0% H_2O ($^C/_N$ = 5.5). UV-visible absorption at 517 nm (Q_1 band) gives a molar extinction coefficient (ε) of 1.6×10^4 M^{-1} cm^{-1}, in agreement with the literature (Kalyanasudaram, 1984). Major IR peaks were observed at 525, 800, 880, 971, 996, 1183, 1214, 1275, 1330, 1355, 1511 and 1636 cm^{-1}. All the other reagents used were of analytical grade and purchased from Merck.

Preparation of Na-saturated clays

With the exception of LPN, all clays were cation-exchanged to the Na-form before saturation with porphyrin. The amount of clay to be treated (100–200 g) was added stepwise to a 5 mol L^{-1} NaCl solution, under mechanical stirring and mild heating (~60ºC). After a period of time that varied from 2 to 7 days, the dispersion was washed with deionized water until it tested negatively for chloride. After the removal of the NaCl excess, the <2 μm clay fraction of SWy-2 and VMC were obtained by sedimentation (Van Olphen, 1977). The Na-exchanged clays were kept as water suspensions in plastic bottles. The concentrations of these dispersions were determined in triplicate and did not show significant changes. The cation exchange capacity (CEC) of SWy-2 and Syn-1 (Na^+-form) was evaluated by a spectrophotometric method using $[Co(NH_3)_6]Cl_3$ as described previously (Dias *et al.*, 2000).

Saturation of the clays with TMPyP

A porphyrin solution was added stepwise, while stirring, to the clays dispersed in deionized water. The amount of TMPyP was calculated considering the clay CEC plus an excess of 5%. The suspension was then refluxed (30–60ºC) for 7 days under stirring and protected from direct light. The porphyrin not immobilized in the clay was removed by centrifugation or dialysis. The solid samples were washed with deionized water until all of the free TMPyP had been removed. This was monitored by UV-visible spectroscopy of the water used in each washing step. After drying (over P_4O_{10}), the amount of TMPyP in the clays was checked by elemental analysis (CHN): SWy-2 – 8.5% C, 1.3% H, 1.8% N; Syn-1 – 5.8% C, 1.7% H, 2.4% N; LPN – 8.7% C, 2.0% H, 2.1% N; VMC – 7.0% C, 2.2% H, 1.5% N. The clay-TMPyP solids were also characterized by UV-visible and Raman spectroscopies.

Characterization

The XRD patterns of oriented samples, prepared by drying aqueous clay suspensions onto glass slides, were recorded using a Philips diffractometer model PW 1710 or model X'Pert-MPD, with CuKα radiation (40 kV and 40 mA) and 2θ varying from 2.5º to 45º (scan step size = 0.02º2θ).

The specific surface area was determined by the N_2-BET method on a QuantaChrome model Quantasorb device. The fraction between 100 and 200 mesh was used in the measurement after heating the sample at 200ºC for 2 h under dynamic N_2 atmosphere.

The UV-visible spectra of the clay-TMPyP aqueous suspensions and also the UV-visible diffuse reflectance spectra of the clay-TMPyP solids (dispersed in $BaSO_4$) were recorded on a Shimadzu UV2401-PC spectrophotometer equipped with an integrating sphere model ISR 240A. UV-visible spectra of solutions were obtained using an Hitachi U-2000 spectrophotometer. Resonance Raman spectra were recorded on a Renishaw Raman Microscope (mod. 3000) fitted with a Peltier cooled CCD detector (600 × 400 pixels, Wright). The 457.9 nm, 488.0 nm and 514.5 nm lines from an Ar^+ laser (Omnichrome) were used to produce the spectra. The laser power was <70 μW at the sample to avoid thermal decomposition.

Thermogravimetric analysis (TGA) experiments were carried out on a Shimadzu TGA-50 equipment under air (flow rate = 50 mL min^{-1}) using a heating rate of 10ºC min^{-1} from ambient temperature to 900ºC. Elemental analysis (CHN) were conducted on a Perkin Elmer 2400 analyzer. The IR spectra were recorded as KBr pellets on a Bomen MB-100, fitted with a DTGS detector, in the range 400–4000 cm^{-1} with a 4 cm^{-1} resolution.

https://doi.org/10.1346/CCMN.2005.0530404 Published online by Cambridge University Press

Table 1. Structural data of the clays: precursor (as received), Na-exchanged and TMPyP saturated.

	CEC ($mmol_c$/100 g)		N_2- BET surface area (m^2/g)			Interlayer spacing, *d*(001) (Å)		
	Precursor	Na	Precursor	Na	TMPyP	Precursor	Na	TMPyP
SWy-2	85[1]	95	22	45	37	11.2[5]	13.0	14.3
Syn-1	n.d.[2]	60	96	103	88	11.2[5]	11.2	12.3
VMC	103 [3]	nd	4	12	17	14.7[3]	15.0	15.5; 20
LPN XLS	50[4]	–	320	–	133	12.7	–	14.4

(1) Borden and Giese (2001); (2) not determined; (3) Coelho (1986);
(4) Laporte; (5) Chipera and Bish (2001)

RESULTS AND DISCUSSION

XRD and physical properties

Experimental data related to the structural characterization of clay samples used in this work are summarized in Table 1. The surface area of the solids decreased when Na^+ ions were replaced by the macrocycle organic cation and, in particular for LPN, the surface area was significantly reduced. It seems that TMPyP intercalation favors the face-to-face clay particles arrangement. The XRD patterns recorded for smectites SWy-2 and LPN showed an increase in basal spacing after the porphyrin intercalation (data not shown). The d_{001} values of 14.3–14.4 Å are in agreement with that reported for TMPyP immobilized into SWy-1 (Carrado and Winans, 1990). TMPyP has dimensions of ~17.5 × 17.5 Å and a thickness of ~4 Å (Giannelis, 1990) which suggest a flat or parallel orientation of the porphyrin ring relative to the inorganic layer.

Considering the carbon percentage in the saturated SWy-2 and LPN samples, the porphyrin concentration in both is ~16 mmol/100 g. The amount of TMPyP in the saturated clay samples could be used to estimate the CEC for comparison with the values reported in Table 1. However, some of the molecules may be protonated (probably as the dication H_2TMPyP) on the clay surfaces, making a CEC evaluation difficult from elemental analysis data. This point will be discussed later in more detail.

The XRD pattern of Na-exchanged Syn-1 (Figure 2) shows that the peak at 7.84°2θ (d = 11.2 Å) has a shoulder at the low-angle side (~5°2θ). A peak at 14.5°2θ (d = 6.1 Å) is attributed to boehmite (Chipera and Bish, 2001). According to the literature (Moll, 2001), Syn-1 is an interstratified 10–12.5 Å phase, where the mica/beidellite ratio is 2, and the interlayer region is occupied by ammonium and hydroxyaluminum ions. TMPyP intercalation is expected only in the expandable beidellite-like space. Upon porphyrin saturation, a broad peak is observed with a maximum at 12.3 Å as well as the low-angle shoulder. Note that the increase in the basal spacing is smaller than that observed for SWy-2 and LPN, but it is still compatible with a TMPyP arrangement parallel to the clay surface. Characterization performed by Wright *et al.* (1972) suggests that mica-like interlayer spaces in Syn-1 are anhydrous and occupied mainly by NH_4^+ ions (hydroxyaluminum ions are probably not present). Elemental analysis data of the Syn-1 sample saturated with TMPyP indicates that porphyrin exchange does not occur to a significant extent in the mica-like interlayer since this synthetic clay has the smallest amount of TMPyP (~11 mmol/100 g) but the highest nitrogen content (for this sample in particular, the nitrogen is provided by the porphyrin and also by ammonium ions).

The XRD patterns of the Na-exchanged VMC sample show very sharp 001 peaks (Figure 2), characteristic of

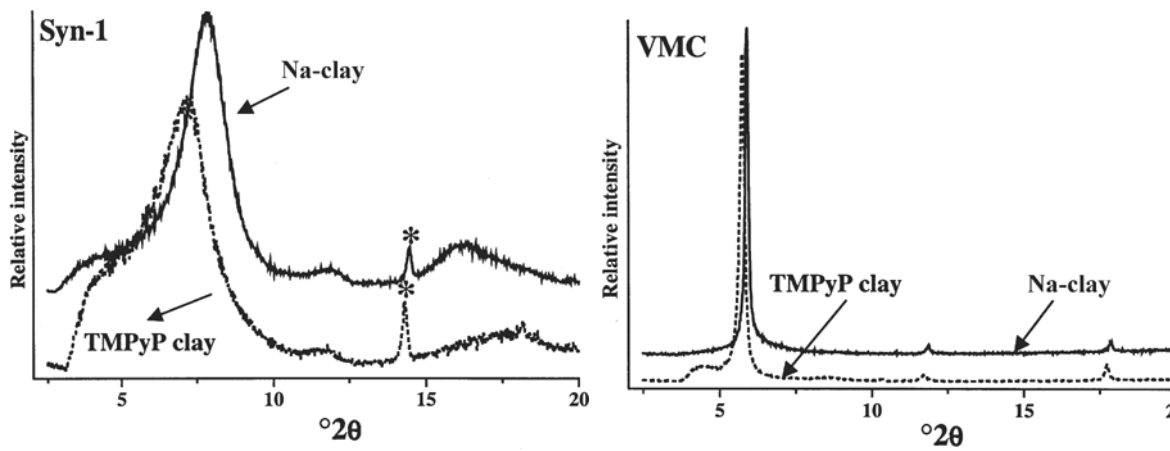

Figure 2. XRD patterns of Syn-1 (left) and VMC (right). Solid line: Na-clay; dotted line: TMPyP saturated clay; (*) boehmite.

https://doi.org/10.1346/CCMN.2005.0530404 Published online by Cambridge University Press

Table 2. Electronic spectroscopy data ($\lambda_{max.}$) of the free base and protonated TMPyP, and the TMPyP saturated clays.

Sample	Diffuse reflectance (nm)	Aqueous suspensions (nm)
TMPyP(1)	423 (S)(2), 522, 561, 603, 660	419 (S), 517, 554, 585, 636
$[H_2TMPyP]^{2+}$ (1)	455 (S), 598, 651	444 (S), 593, 643
LPN XLS	431 (sh)(2)/462 (S), 603	423 (S)/454 (sh), 487, 545, 584, 611
VMC	430 (S)/457 (sh), 533, 596, 654	420 (S)/ 455 (sh), 526, 592, 659
Syn-1	430 (sh)/465 (S), 595, 632, 678	452 (S), 539, 583, 616, 669
SWy-2	432 (sh)/468 (S)/491 (sh), 617, 705	458 (S) / 487 (sh), 612

(1) TMPyP as chloride salt; protonated porphyrin in the solid state was obtained through the evaporation of a 1 mol/L HCl solution containing TMPyP; (2) (S) and (sh) indicate the Soret band and a shoulder, respectively; all the Q bands (>500 nm) are very broad for the intercalates

the well ordered layer stacking of this clay mineral. When the Na^+ ion is replaced by TMPyP, sharp peaks are also observed and the basal spacing increases to 15.5 Å. The similarity between the XRD patterns suggests that TMPyP is not intercalated between the layers, but rather sorbed only at the external surfaces. However, considering the small BET surface area of this clay (17 m^2/g) it is difficult to explain the relatively large amount of porphyrin found in the saturated system (13.3 mmol/100 g) on the basis of sorption at the external clay surfaces alone. A simple calculation using the porphyrin area (17.5 × 4 Å), the clay BET area (17 m^2/g) and assuming a perpendicular arrangement of TMPyP at the external surface gives 4 mmol/100 g as the maximum amount of porphyrin in such a system. This value is <1/3 of the total amount of TMPyP, as determined by elemental analysis (13.3 mmol/100 g), indicating that the majority of the molecules should be intercalated between the VMC layers. The small change in basal spacing (Δd = 0.5 Å) indicates a flat orientation of the porphyrin in the interlayer space. In addition to the sharp peaks, the XRD pattern of the VMC-TMPyP sample shows a weak and broad peak at ~3.8–4.8°2θ ($d \approx$ 23.8–17.8 Å) suggesting the presence of tilted porphyrin molecules between the silicate layers. The peak broadness indicates a range of orientations that may be a consequence of the charge heterogeneity of vermiculites (Peréz-Rodrígues and Maqueda, 2002).

Spectroscopic characterization by resonance Raman

The electronic spectrum of porphyrins is dominated by a strong band ($\varepsilon \approx 10^5\ cm^{-1}\ M^{-1}$) around the 380–450 nm region (referred to as the Soret band) and a set of weaker bands ($\varepsilon \approx 10^4\ cm^{-1}M^{-1}$) at longer wavelengths (500–700 nm) known as Q bands (Gouterman, 1978; Milgrom, 1997). These absorption bands arise from $\pi \rightarrow \pi^*$ electronic transitions. Under the D_{2h} symmetry (as in the free base) four Q bands are expected in the visible spectrum but in protonated or metallated porphyrins, the molecular symmetry changes to D_{4h} and only two Q bands are observed. Table 2 shows the absorption maxima of the Soret and Q bands of the free base and protonated TMPyP.

In general, when TMPyP interacts with clays a significant red shift is observed in the UV-visible electronic spectrum obtained in the solid state (Carrado and Winans, 1990; Dias *et al*., 2000) or as aqueous colloidal dispersions (Kuykendall and Thomas, 1990; Chernia and Gill, 1999; Takagi *et al*., 2002a, 2002b). Other inorganic matrices such as mesoporous aluminosilicate in contact with porphyrin also present similar behavior (Sung-Suh *et al*., 1997).

Figure 3 shows the UV-visible diffuse reflectance spectra of the solids VMC-TMPyP, LPN-TMPyP, SWy-2-TMPyP and Syn-1-TMPyP dispersed in $BaSO_4$ where red shifts of the Soret and Q bands are clearly observed. Furthermore, the Soret band broadens and in some cases a structure is defined (shoulders at ~430 nm and 490 nm), indicating the presence of different chemical species and/or distinct environments. Another interesting feature is the high relative intensity of the Q bands, suggesting that the transition moments are substantially affected by the surrounding environment.

When the UV-visible spectra are recorded from the isolated solids suspended in water (Figure 4), the bands are better resolved and at least three different compo-

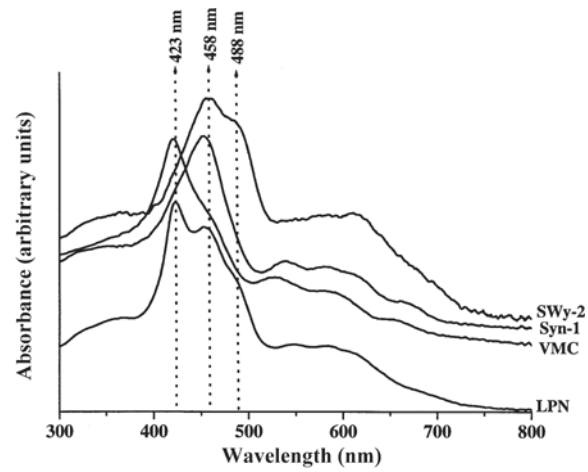

Figure 3. Diffuse reflectance spectra of TMPyP free base and of the protonated form and also of the clays saturated with TMPyP. The arrows indicate the position of the laser lines used to produce the Raman spectra.

https://doi.org/10.1346/CCMN.2005.0530404 Published online by Cambridge University Press

nents are evident in the Soret region, with the absorption maximum showing up at ~425 nm, 460 nm and 480 nm. Table 2 presents the UV-visible absorption bands positions for the samples in the solid state and also when suspended in water.

From Figure 4, it can be concluded that the shape of the Soret band is determined by the relative contribution of several components. VMC-TMPyP, for example, does not display the long-wavelength absorption (~480 nm) in the spectrum of the aqueous suspension, whereas for SWy-2-TMPyP it is nearly as strong as the 460 nm band (Figure 4). The red shift of the TMPyP Soret band increases in the order VMC < LPN < Syn-1 < SWy-2 for aqueous suspensions. The bands in the spectra of solid dry samples are much broader and not so clearly resolved, thus, curve fitting is much more complex and the differences in the spectra are more subtle and difficult to define (compare for example the spectra of LPN-TMPyP and Syn1-TMPyP in Figure 3). Nevertheless, a trend for the red shift in the solids can be proposed: VMC < LPN ≈ Syn-1 < SWy-2 (study of samples dispersed in water is out of the scope of the present investigation).

Concerning the red shift observed in the TMPyP-clay spectra (dried solids or in aqueous suspension), the literature reports the possibility of protonation of the porphyrin ring nitrogens (Carrado and Winans, 1990; Kuykendall and Thomas, 1990) or *Me*Py substituent rotation towards planarity (Chernia and Gill, 1999). Carrado and Winans (1990) also discussed the bathochromic shift in the spectrum of TMPyP intercalated in montmorillonite as a consequence of protonation that would lead to a "more planar structure". This point deserves more detailed discussion.

Stone and Fleischer (1968) used XRD analysis to determine the structure of meso-tetraphenylporphine (TPP) and meso-tetra(4-pyridyl)porphine (TPyP) diacids

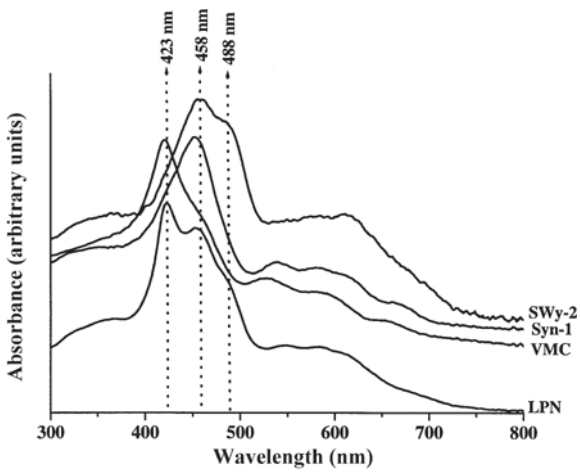

Figure 4. Absorption electronic spectra of the aqueous dispersions of the clays saturated with TMPyP. The arrows indicate the position of the Soret band.

and found that protonation causes out-of-plane distortion of the porphyrin ring, probably as a consequence of repulsion of the positively charged nitrogen atoms in the porphyrin core and/or steric hindrance if the four hydrogen atoms were coplanar. However, the relationship between the observed XRD pattern and the red shift (~30 nm for TPyP) in the Soret band upon protonation was not clearly established by the authors. Generally, a more extended conjugation is expected to increase the electronic stability of a molecule, thus leading to red shifted electronic transitions. In the case of TMPyP, where the *Me*Py groups are nearly perpendicular to the porphyrin ring, a larger conjugation would demand a rotation of the substituent rings towards a more planar arrangement. It is thus tempting to ascribe the behavior of the electronic spectrum of TMPyP when interacting with acidic clays to protonation and thus to planarity, based on the observed red shift. It must be emphasized, however, that such rationale finds no support in the XRD data as reported by Stone and Fleischer (1968).

A decrease in the dihedral angle formed between the free base (non-protonated) porphyrin ring and the *Me*Py substituent also causes a red shift according to calculations (Chernia and Gill, 1999), but in the ground state such rotation is hindered by the hydrogen atoms bounded to C_β. This causes a large energy change when the substituent groups are rotated from the 90° arrangement. Monaco and Zhao (1993) have also shown that the substituent rotation causes a concomitant deformation of the porphyrin ring.

On the other hand, theoretical calculations performed considering metallated meso-substituted porphyrins have shown that distortions caused by voluminous groups at the meso position causes an increase in both HOMO and LUMO energies. However, the HOMO is more affected than the LUMO, leading to a red-shifted electronic transition (Takeuchi *et al.*, 1994). This result finds support in the conclusion drawn from time-resolved resonance Raman spectroscopy (TR^3) wherein, in the excited state, the porphyrin core expands due to a larger $C_\alpha - C_m$ distance (Kumble *et al.*, 1995). If this applies to TMPyP, the excited state would be less perturbed by the substituent rotation than the ground state and the increase in the orbital energy with distortion would be smaller in the excited than in the ground state, explaining the observed red shift for the protonated TMPyP. At this point it is interesting to emphasize that solvent polarity, which is usually an important factor concerning HOMO and LUMO energies, was discarded since TMPyP appears to be insensitive to solvent polarity (Kuykendall and Thomas, 1990).

Considering that TMPyP protonation, porphyrin ring out-of-plane distortion and meso-substituent rotation are all able to cause the observed red shifts, no conclusion can be drawn from the UV-visible electronic absorption spectra alone. Unfortunately, the information obtained from the spectra of solids or suspensions (peak positions and

https://doi.org/10.1346/CCMN.2005.0530404 Published online by Cambridge University Press

bandwidths) is not specific, and definitive identification of the species responsible for the electronic transitions is not possible. This is true especially for the LPN-TMPyP system, which has been the subject of some controversy in the literature concerning the interpretation of its UV-visible absorption spectrum: Kuykendall and Thomas (1990) concluded that the porphyrin was protonated at the LPN surface, while Chernia and Gill (1999) used strong arguments to propose *Me*Py rotation instead of protonation.

Resonance Raman spectroscopy has proved to be a very useful tool in the investigation of porphyrin-clay systems (Dias *et al*., 2000); a wider range of applications of Raman spectroscopy in the study of catalysts was published recently (Wachs, 2001). It is also employed here to provide an improved understanding of the reasons for the shift and broadening of the Soret band.

The Raman spectra were recorded, exciting the clay samples at 457.9 nm, 488.0 nm and 514.5. These lines were chosen according to the absorption band positions listed in Table 2. The vibrational modes associated with the chromophoric groups, therefore, will be selectively enhanced for each of the three absorptions in the Soret region. Since resonance Raman spectroscopy is sensitive to protonation, distortions and environment effects, as mentioned above, excitation at the maximum of the absorption bands (or close to) permits an unequivocal assignment of the chromophoric species.

Figures 5, 6 and 7 show the Raman spectra of the porphyrin-clay samples excited at 457.9 nm, 488.0 nm and 514.5 nm, respectively. These lines are in resonance with the strong Soret absorption at ~460 nm and 490 nm (see Figure 3), and are expected to provide information on the nature of the porphyrin-clay interactions. Although there is no resonance Raman data for the ~430 nm absorption, it seems reasonable to assume that it corresponds to TMPyP adsorbed on the external surfaces of the inorganic matrices as it is very close to the observed value for the free base itself.

In previous work (Dias *et al.*, 2000), it was shown that the most significant change in the resonance Raman spectrum of the diprotonated TMPyP is a down shift of ~15 cm^{-1} in the 1550 cm^{-1} band (ν C_β–C_β) when compared to the free base (Figure 8); the other features observed in the spectrum of the diacid species in the 900–1400 cm^{-1} region are not protonation band markers as they also appear when the molecular symmetry changes. Molecular geometry distortions caused by the confinement can also be probed since they promote a reduction in the molecular symmetry, causing an increase in the number of observed bands.

Comparing the Raman spectra presented in Figure 5 (excited at 457.9 nm), the most important aspects are the evolution of features characteristic of the protonated porphyrin and the relative intensity of the *Me*Py bands. In the first case, it is observed that the VMC and LPN samples do not cause any significant perturbation in the resonance Raman spectrum of the porphyrin as compared to the free base. Particularly in the case of VMC, there is no indication of protonation that can be followed by the behavior of the band around 1550 cm^{-1} (in LPN, the bandwidth suggests a small contribution of the diacid). On the other hand, when the porphyrin interacts with SWy-2 it is possible to distinguish in its Raman

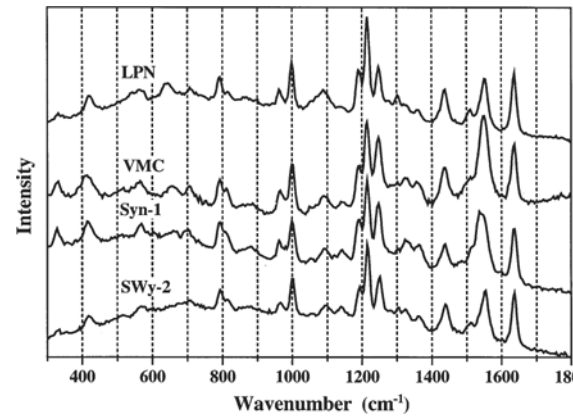

Figure 6. Resonance Raman spectra of the clays saturated with TMPyP, $\lambda_{exc.}$ = 488.0 nm.

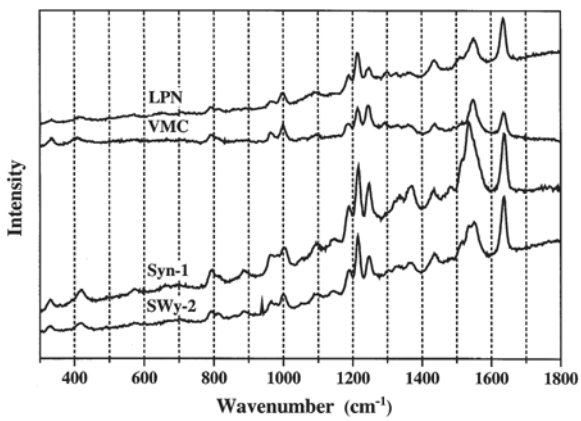

Figure 5. Resonance Raman spectra of the clays saturated with TMPyP, $\lambda_{exc.}$ = 457.9 nm.

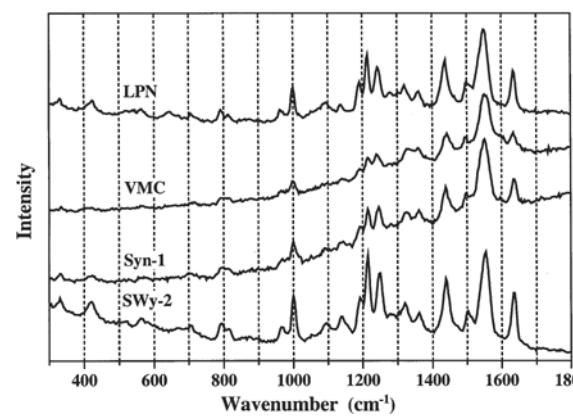

Figure 7. Resonance Raman spectra of the clays saturated with TMPyP, $\lambda_{exc.}$ = 514.5 nm

https://doi.org/10.1346/CCMN.2005.0530404 Published online by Cambridge University Press

spectrum the presence of two bands in the 1550 cm^{-1} region. One of these (1550 cm^{-1}) can be assigned to the non-protonated porphyrin and the other (1536 cm^{-1}) to the diacid form (see Figure 8). In the Syn-1-TMPyP system the 1536 cm^{-1} dominates the spectrum, hampering the much weaker free base counterpart. Other minor changes associated with protonation, such as changes in the relative intensities of the bands in the 1200 and 1350 cm^{-1} regions, are also observed. Accordingly, the behavior of the Raman spectra excited at 457.9 nm suggests the following clay acidity order for the samples (all dried and stored under the same conditions): VMC < LPN < SWy-2 < Syn-1.

A search of the literature revealed that the acidity of several clays can be evaluated using dyes such as methylene blue and thionine (Cenens and Schoonheydt, 1988; Neumann *et al.*, 1996; Jacobs and Schoonheydt, 1999; Jacobs and Schoonheydt, 2001). According to these studies, Laponite has less acidity than montmorillonites SWy-2 and Syn-1, with Syn-1 being more acidic. The contribution of clay properties (such as octahedral or tetrahedral substitution, particle size, surface area, acidity *etc.*) was addressed by Jacobs and Schoonheydt (2001) in their investigation of dye speciation in different aluminosilicates. Therefore the acidic order observed in this work is in agreement with data reported in the literature using other dyes. It must be emphasized, however, that the Jacobs and Schoonheydt (2001) studies were carried out in aqueous dispersion whereas our results were obtained for dried solid samples. The complementary Raman investigation of water suspensions is currently under way.

Clearly, LPN has less acidity than SWy-2 and Syn-1. It is important to point out here that their reflectance spectra are similar, but this is not the case when resonance Raman spectroscopy is used. These data give credence to the use of resonance Raman spectroscopy as a very powerful tool in the identification of chemical species adsorbed or intercalated on clays. From the 1550 cm^{-1} bandwidth, a contribution from the diprotonated TMPyP can be anticipated in LPN, but certainly it is not the most significant species, reinforcing the arguments used by Chernia and Gill (1999).

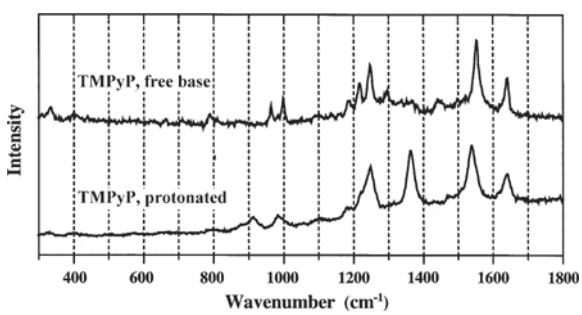

Figure 8. Resonance Raman spectra of the porphyrin TMPyP (solid state), free base and protonated, $\lambda_{exc.}$ = 457.9 nm.

Further evidence is given by the relative intensity of the *Me*Py modes, which suggests a larger electronic delocalization as discussed below. Note that this does not mean that TMPyP is in a planar structure but only that a decrease in the dihedral angle is occurring.

The more acidic clay is Syn-1, and here the *Me*Py relative intensities are much smaller than in LPN and SWy-2. It seems plausible to consider that diprotonation of the central nitrogen rings changes both the electronic and spatial porphyrin structures, such that the larger flexibility promoted by the interaction with the surface is now hindered. It must be remembered that (1) protonation causes a distortion in the porphyrin ring structure in order to accommodate the two positive charges (such distortion was verified by Stone and Fleischer (1968) for TPP and TPyP); and (2) the distortion promoted by protonation is not enough to remove the D_{4h} symmetry (resonance Raman spectrum and electronic absorption spectrum agree with this assumption, because in the former a decrease in the overall symmetry is not detected whereas in the latter the Q band region shows only two bands, consistent with D_{4h} symmetry).

The Raman spectrum obtained for VMC-TMPyP is very similar to the free base porphyrin, in agreement with the electronic spectrum of the suspension that indicated an insignificant amount of protonated TMPyP at VMC surfaces. Such behavior may be explained by the larger contribution of tetrahedral substitution in VMC when compared to the other clays; it has been argued that octahedral substitution enhances the acidity at the clay surface (Yariv, 1992).

As mentioned above, besides protonation processes, the resonance Raman spectra in Figure 5 (excited at 457.9 nm) reveal modifications in the relative intensity of the *Me*Py bands. The substituent bands are enhanced (particularly in the LPN-TMPyP spectrum) and the most striking ones are the ~1635 cm^{-1} and the ~1215 cm^{-1} modes, both involving the methyl-pyridyl (*Me*Py) substituent (ν(C=C) + ν(C=N) and $\nu(C_m-C_{MePy})$, respectively). As it is very difficult to use a reliable internal standard for intensity, relative values were estimated using a porphyrin band at 1190 cm^{-1} which is not significantly affected by the excitation wavelength. The relative intensity of the enhanced *Me*Py modes can be arranged as LPN > SWy-2 > Syn-1 > VMC.

When excitation is performed at 488.0 nm (where free base and protonated TMPyP do not absorb), the band at ~1550 cm^{-1} (non-protonated species) predominates over the 1536 cm^{-1} (protonated porphyrin) for all the investigated systems and several bands are enhanced below 1000 cm^{-1} where out-of-plane vibrations are expected. Except in the case of Syn-1 where the contribution of the diacid is still observed (albeit much weaker than at 457.9 nm), the recorded data indicate that the absorption band at ~480 nm corresponds to an electronic transition of a non-protonated species.

https://doi.org/10.1346/CCMN.2005.0530404 Published online by Cambridge University Press

Furthermore, the increase in the number of enhanced modes suggests a lowering in the molecular symmetry caused by the interaction with the clay surface. These modes are mostly out-of-plane vibrations, strongly suggesting a distortion of the porphyrin ring from planarity. So the long-wavelength component of the Soret band consists of a distorted form of the porphyrin ring, such that the D_{2h} symmetry is lowered, probably to C_{2v}. In this case, A_1 vibrations (in the new symmetry) originate from both A_g and B_{1u} vibrations (in the D_{2h} symmetry) and are expected to be enhanced under resonance conditions. An assignment for the low-frequency bands is not straightforward because the majority of resonance Raman data for TMPyP use excitation within the Soret band and, accordingly, only the totally symmetric vibrations are enhanced with very few being observed below 900 cm^{-1}. The VMC-TMPyP displays the most intense enhancement of the out-of-plane modes.

The enhancement of out-of-plane vibrations in the resonance Raman spectra of the clay-porphyrin systems is an unequivocal indication that macrocycle distortion from planarity occurs when it is intercalated in the clay galleries. The results obtained using 488.0 nm excitation is in agreement with the proposal by Chernia and Gill (1999).

It is not clear, however, if the porphyrin ring distortion is a consequence of steric hindrance or any other property of the restricted environment. The structural distortion might be a consequence of a porphyrin conformation that maximizes the interactions with the inorganic host. Kuykendall and Thomas (1990) proposed that, besides protonation, the red shift of the TMPyP Soret band in clay colloidal dispersions could be due to a distortion in the porphyrin ring caused by the electrostatic attraction between the *Me*Py substituent and the clay charges. We can thus visualize two processes concerning the TMPyP-clay interaction: (1) the porphyrin protonation provokes the core distortion facilitating the *Me*Py rotation (such rotation would be less hindered by the hydrogen atoms bounded to C_β); and (2) the porphyrin confinement between the clay layers induces the *Me*Py rotation and, consequently, the macrocycle ring distortion from planarity.

We are not sure whether confinement is the only effect responsible for the species absorbing at ~490 nm (non-planar porphyrin), or whether adsorption at the external surfaces of the clays with high charge density is also important. The data (out-of-plane vibrations present larger relative intensities in VMC) show that a larger amount of non-planar macrocycles is observed in vermiculite than in smectites, which could be a consequence of the greater layer-charge density in the former. This point is currently under investigation in our laboratory.

Besides the spectral changes, non-planar deformations also affect the porphyrin basicity, $\pi-\pi$ aggregation and metallation processes (Shelnutt *et al.*, 1998). Therefore, the non-planarity caused by the macrocycle interaction with the clay environment can reveal new physical and chemical properties for the porphyrin, providing an opportunity to evaluate as yet unexplored applications.

From the Raman data collected at 457.9 nm and 488.0 nm, it can be concluded that at least two different processes are likely to occur: protonation of the free base and distortion of the non-protonated porphyrin ring. Finally, as SWy-2 displays the largest red shift in its reflectance spectrum, when excited at 514.5 nm it will be at the same resonance conditions as displayed by the other clay-porphyrin systems excited at 488.0 nm (see Figure 3). This is the reason for the large enhancement of the out-of-plane vibrations in SWy-2-TMPyP when excited at 514.5 nm.

If excitation is performed in the green (514.5 nm), a resonance occurs with the first Q band (except in the case of SWy-2 as discussed above) which corresponds to an allowed transition. The same considerations as in the case of the 457.9 nm excitation thus apply except for the fact that the contribution of the diprotonated species is expected to be significantly smaller, since the Q bands in the diacid appears at a much lower energy (593 and 643 nm). In fact, the experimental data agree with such an assumption, and the out-of-plane modes as well as the features for the diprotonated species are barely seen.

CONCLUSIONS

Resonance Raman spectroscopy was used to investigate the TMPyP interaction with VMC, LPN, SWy-2 and Syn-1. Electronic absorption spectra clearly show three distinct Soret bands and it was possible to selectively excite two of them, with laser lines at 457.9 and 488.0 nm. Excitation at 457.9 nm indicated that the absorption band at ~460 nm observed in the TMPyP-Syn-1 system corresponds to a transition of the diprotonated porphyrin, whereas for LPN-TMPyP and VMC-TMPyP, it corresponds to a non-protonated species presenting a smaller dihedral angle between the porphyrin ring and *Me*Py substituent compared to the free TMPyP. The SWy-2-TMPyP system appears to contain both species. Therefore we can say that two TMPyP species are responsible for the absorption at ~460 nm in the UV-visible spectra and resonance Raman is a technique that allows their identification. The nature of these two species (protonated or non-protonated presenting a smaller dihedral angle) depends on the clay properties such as acidity.

In addition, excitation at 488.0 nm clearly shows that the low-energy absorption (at ~490 nm) can be assigned to an electronic transition of the out-of-plane distorted free base porphyrin. The confinement effect may be responsible for the TMPyP ring distortion but other parameters (layer-charge density for example) deserve further investigations.

https://doi.org/10.1346/CCMN.2005.0530404 Published online by Cambridge University Press

Excitation at 514.5 nm was used to confirm the information obtained when the 457.9 nm and 488.0 nm laser lines were used. In the case of the SWy-2-TMPyP system (which presents the largest red shift in the UV-visible absorption bands), the Raman spectrum produced at 514.5 nm provides the same information as the 488.0 nm line does for the other samples. Furthermore, except for SWy-2, at 514.5 nm there is no enhancement of the out-of-plane modes, reinforcing the assignment of the absorption band at ~490 nm to a transition of the distorted porphyrin.

It was shown that electronic absorption spectroscopy alone cannot address the problem of identification of chemical species present in the porphyrin/clay systems studied as it is a non-specific technique. Raman spectroscopy can provide molecular structure identification and with a suitable choice of the excitation line it is possible to enhance some vibrational modes of specific chromophoric groups selectively (resonance Raman), thus allowing its unequivocal assignment.

Raman spectroscopy was used successfully here in the characterization of the chemical species formed when TMPyP interacts with clays which have different properties. Protonation, ring distortion and rotation of the meso substituent were responsible for the specific changes in the Raman spectrum when compared to the pure porphyrin spectrum.

ACKNOWLEDGMENTS

The authors are indebted to the Brazilian agencies Fapesp (Fundação de Amparo à Pesquisa do Estado de São Paulo) and CNPq (Conselho Nacional de Desenvolvimento Científico e Tecnológico) for research grants. We also acknowledge Prof. Antonio Carlos V. Coelho (Escola Politécnica – USP) and Laporte Inorganics for providing the VMC and LPN samples, respectively. Our thanks to Dr Randall T. Cygan, Dr Kathleen Carrado and the other two unknown referees for suggestions that helped to improve this paper.

REFERENCES

Alberti, G. and Costantino, U. (1996) Layered solids and their intercalation chemistry. Pp. 1–23 in: *Solid-State Supramolecular Chemistry: Two- and Three-Dimensional Inorganic Networks* vol. **7** (G. Alberti and T. Bein, editors). Pergamon, New York.

Albrecht, A.C. (1961) Theory of Raman intensities. *Journal of Chemical Physics*, **34**, 1476–1484.

Baker, E.W. and Palmer, S.E. (1978) Geochemistry of porphyrins. Pp. 485–551 in: *The Porphyrins* vol. **1** (D. Dolphin, editor). Academic Press, New York.

Bedioui, F. (1995) Zeolite-encapsulated and clay-intercalated metal porphyrin, phthalocyanine and Schiff-base complexes as models for biomimetic oxidation catalysts – An overview. *Coordination Chemistry Reviews*, **144**, 39–68.

Bergaya, F. and Van Damme, H. (1982) Stability of metalloporphyrins adsorbed on clays – A comparative study. *Geochimica et Cosmochimica Acta*, **46**, 349–360.

Borden D. and Giese, R.F. (2001) Baseline studies of the Clay Minerals Society source clays: Cation exchange capacity measurements by the ammonia-electrode method. *Clays and Clay Minerals*, **49**, 444–445.

Cady, S.S. and Pinnavaia, T.J. (1978) Porphyrin intercalation in mica-type silicates. *Inorganic Chemistry*, **17**, 1501–1507.

Carrado, K.A. and Winans, R.E. (1990) Interactions of water-soluble porphyrins and metalloporphyrins with smectite clay surfaces. *Chemistry of Materials*, **2**, 328–335.

Carrado, K.A. and Wasserman, S.R. (1996) Stability of Cu(II)- and Fe(III)-porphyrins on montmorillonite clay: an X-ray absorption study. *Chemistry of Materials*, **8**, 219–225.

Carrado, K.A., Anderson, K.B. and Grutkoski, P.S. (1992) Thermal analysis of porphyrin-clay complexes. Pp. 155–165 in: *Supramolecular Architecture – Synthetic Control in Thin Films and Solids* (T. Bein, editor). ACS Symposium Series, Washington D.C.

Cenens, J. and Schoonheydt, R.A. (1988) Visible spectroscopy of methylene blue on hectorite, laponite B, and barasym in aqueous suspension. *Clays and Clay Minerals*, **36**, 214–224.

Chernia, Z. and Gill, D. (1999) Flattening of TMPyP adsorbed on laponite. Evidence in observed and calculated UV-vis spectra. *Langmuir*, **15**, 1625–1633.

Chibwe, M., Ukrainczyk, L., Boyd, S.A. and Pinnavaia, T.J. (1996) Catalytic properties of biomimetic metallomacrocycles intercalated in layered double hydroxides and smectite clay: the importance of edge-site access. *Journal of Molecular Catalysis*, **113A**, 249–256.

Chipera, S.J. and Bish, D.L. (2001) Baseline studies of the Clay Minerals Society source clays: Powder X-ray diffraction analyses. *Clays and Clay Minerals*, **49**, 598–409.

Coelho, A.C.V. (1986) Estudo, em escala de laboratório, do inchamento em água de vermiculitas brasileiras tratadas com soluções salinas inorgânicas. Master Dissertation, Universidade de São Paulo, São Paulo, Brazil, 244 pp.

Dias, P.M., de Faria, D.L.A. and Constantino, V.R.L. (2000) Spectroscopic studies on the interaction of tetramethylpyridylporphyrins and cationic clays. *Journal of Inclusion Phenomena and Macrocyclic Chemistry*, **38**, 251–266.

Drain, C.M., Gentemann, S., Roberts, J.A., Nelson, N.Y., Medforth, C.J., Jia, S.L., Simpson, M.C., Smith, K.M., Fajer, J., Shelnutt, J.A. and Holten, D. (1998) Picosecond to microsecond photodynamics of a non-planar nickel porphyrin: Solvent dielectric and temperature effects. *Journal of the American Chemical Society*, **120**, 3781–3791.

Giannelis, E.P. (1990) Highly organized molecular assemblies of porphyrin guest molecules in mica-type silicates – Influence of guest host interactions on molecular-organization. *Chemistry of Materials*, **2**, 627–629.

Gouterman, M. (1978) Optical spectra and electronic structure of porphyrins and related rings. Pp. 1–165 in: *The Porphyrins* vol. **3** (D. Dolphin, editor). Academic Press, New York.

Jacobs, K.Y. and Schoonheydt R.A. (1999) Spectroscopy of methylene blue-smectite suspensions. *Journal of Colloid and Interface Science*, **220**, 103–111.

Jacobs, K.Y. and Schoonheydt R.A. (2001) Time dependence of the spectra of methylene blue-clay mineral suspensions. *Langmuir*, **17**, 5150–5155.

Kalyanasundaram, K. (1984) Photochemistry of water-soluble porphyrins – comparative study of isomeric tetrapyridyl(N-methylpyridiniumyl)porphyrin and tetrakis(N-methylpyridiniumyl)porphyrins. *Inorganic Chemistry*, **23**, 2453–2459.

Kaufherr, N., Yariv, S. and Heller, L. (1971) Effect of exchangeable cations on sorption of chlorophyllin by montmorillonite. *Clays and Clay Minerals*, **19**, 193–200.

Kosiur, D.R. (1977) Porphyrin adsorption by clay-minerals. *Clays and Clay Minerals*, **25**, 365–371.

Kumble, R., Loppnow, G.R., Hu, S.Z., Mukherjee, A., Thompson, M.A. and Spiro, T.G. (1995) Studies of the vibrational and electronic-structure of the S1 excited states of beta-substituted porphyrins by picosecond time-resolved

resonance Raman spectroscopy. *Journal of Physical Chemistry*, **99**, 5809–5816.

Kuykendall, V.G. and Thomas, J.K. (1990) Photophysical investigation of the degree of dispersion of aqueous colloidal clay. *Langmuir*, **6**, 1350–1356.

Laporte, Inc. (Widnes, UK) *Laponite, The Technical Directory*, 24 pp.

Martinez-Lorente, M.A., Battioni, P., Kleemiss, W., Bartoli, J.F. and Mansuy, D. (1996) Manganese porphyrins covalently bound to silica and montmorillonite K10 as efficient catalysts for alkene and alkane oxidation by hydrogen peroxide. *Journal of Molecular Catalysis*, **113A**, 343–353.

Milgrom, L.R. (1997) *The Colours of Life – an Introduction to the Chemistry of Porphyrins and Related Compounds*. Oxford University Press, New York, 249 pp.

Moll Jr., W.F. (2001) Baseline studies of the Clay Minerals Society source clays: Geological origin. *Clays and Clay Minerals*, **49**, 374–380.

Monaco, R.R and Zhao, M. (1993) Computational studies of peripheral ring twisting in meso-N-methyl pyridyl-substituted porphyrins. *International Journal of Quantum Chemistry*, **46**, 701–709.

Neumann, M.G., Schmitt, C.C. and Gessner, F. (1996) Time-dependent spectrophotometric study of the interaction of basic dyes with clays II: Thionine on natural and synthetic montmorillonites and hectorites. *Journal of Colloid and Interface Science*, **177**, 495–501.

Onaka, M., Shinoda, T., Izumi, Y. and Nolen, E. (1993) Clay-mediated meso-tetraarylporphyrin synthesis. *Tetrahedron Letters*, **34**, 2625–2628.

Pérez-Rodríguez, J.L. and Maqueda, C. (2002) Interactions of vermiculites with organic compounds. Pp. 113–173 in: *Organo-clay Complexes and Interactions* (S. Yariv and H. Cross, editors). Marcel Dekker, New York.

Rouxel, J., Tournoux, M. and Brec, R., editors (1994) Soft Chemistry Routes to New Materials – Chimie Douce. *Materials Science Forum*, v. **152–153**. Trans Tech Publications Ltd., Switzerland, 402 pp.

Shelnutt, J.A., Medforth, C.J., Berber, M.D., Barkigia, K.M. and Smith, K.M. (1991) Relationships between structural parameters and Raman frequencies for some planar and non-planar Nickel(II) porphyrins. *Journal of the American Chemical Society*, **113**, 4077–4087.

Shelnutt, J.A., Song, X., Ma, J., Jia, S., Jentzen, W. and Medforth, C.J. (1998) Non-planar porphyrins and their significance in proteins. *Chemical Society Reviews*, **27**, 31–41.

Stone, A. and Fleischer, E.B. (1968) The molecular and crystal structure of porphyrin diacids. *Journal of the American Chemical Society*, **90**, 2735–2748.

Sun, J., Chang, C.K. and Loehr, T.M. (1997) Q-band resonance Raman enhancement of Fe-CO vibrations in ferrous chlorin complexes: Possible monitor of axial ligands in d cytochromes. *Journal of Physical Chemistry B*, **101**, 1476–1483.

Sung-Suh, H.M., Luan, Z. and Kevan, L. (1997) Photoionization of porphyrins in mesoporous siliceous MCM-41, AlMCM-41, and TiMCM-41 molecular sieves. *Journal of Physical Chemistry B*, **101**, 10455–10463.

Takagi, S., Tryk, D.A. and Inoue, H. (2002a) Photochemical energy transfer of cationic porphyrin complexes on clay surface. *Journal of Physical Chemistry B*, **106**, 5455–5460.

Takagi, S., Shimada, T., Eguchi, M., Yui, T., Yoshida, H., Tryk, D.A. and Inoue, H. (2002b) High-density adsorption of cationic porphyrins on clay layer surfaces without aggregation: The size-matching effect. *Langmuir*, **18**, 2265–2272.

Takeuchi, T., Gray, H.B. and Goddard, W.A., III (1994) Electronic structures of halogenated porphyrins: spectroscopic properties of ZnTFPPX8 (TFPPX8= Ocata-B-halotetrakis(pentafluorophenyl)porphyrin; X=Cl, Br). *Journal of the American Chemical Society*, **116**, 9730–9732.

Ukrainczyk, L., Chibwe, M., Pinnavaia, T.J. and Boyd, S.A. (1994) Esr study of Cobalt(II) tetrakis(N-methyl-4-pyridiniumyl)porphyrin and Cobalt(II) tetrasulfophthalocyanine intercalated in layered aluminosilicates and a layered double hydroxide. *Journal of Physical Chemistry*, **98**, 2668–2676.

Ukrainczyk, L., Chibwe, M., Pinnavaia, T.J. and Boyd, S.A. (1995) Reductive dechlorination of carbon-tetrachloride in water catalyzed by mineral supported biomimetic cobalt macrocycles. *Environmental Science & Technology*, **29**, 439–445.

Unger, E., Dreybrodt, W. and SchweitzerStenner, R. (1997) Conformational properties of nickel(II) meso-tetraphenylporphyrin in solution. Raman dispersion spectroscopy reveals the symmetry of distortions for a non-planar conformer. *Journal of Physical Chemistry A*, **101**, 5997–6007.

Van Damme, H., Crespin, M., Obrecht, F., Cruz, M.I. and Fripiat, J.J. (1978) Acid-base and complexation behavior of porphyrins on intra-crystal surface of swelling clays – Meso-tetraphenylporphyrin and meso-tetra(4-pyridyl)porphyrin on montmorillonites. *Journal of Colloid and Interface Science*, **66**, 43–54.

Van Olphen, H. (1977) *An Introduction to Clay Colloid Chemistry: for Clay Technologists, Geologists and Soil Scientists*, 2nd edition. John Wiley & Sons, New York.

Wachs, I.E. (2001) Raman Spectroscopy of Catalysts. Pp. 799–833 in: *Handbook of Raman Spectroscopy – From the Research Laboratory to the Process Line* (I.R. Lewis and H.G.M. Edwards, editors). Marcel Dekker, New York.

Wright, A.C., Granquist, W.T. and Kennedy, J.V. (1972) Catalysis by layer silicates. I. The structure and thermal modification of a synthetic ammonium dioctahedral clay. *Journal of Catalysis*, **25**, 65–80.

Yariv, S. (1992) The effect of tetrahedral substitution of Si by Al on the surface acidity of the oxygen plane of clay minerals. *International Review in Physical Chemistry*, **11**, 345–375.

(*Received 23 June 2003; revised 2 February 2005; Ms. 807; A.E. Randall T. Cygan*)